

# HEAVY QUARK PHOTOPRODUCTION IN THE SEMIHARD QCD APPROACH AND THE UNINTEGRATED GLUON DISTRIBUTION

**A.V. Lipatov**<sup>1</sup>

*Department of Physics,  
M.V. Lomonosov Moscow State University,  
119899 Moscow, Russia*

**V.A. Saleev**<sup>2</sup>

*Department of Physics,  
Samara State University,  
443011 Samara, Russia*

**N.P. Zotov**<sup>3</sup>

*D.V. Skobeltsyn Institute of Nuclear Physics,  
M.V.Lomonosov Moscow State University,  
119899 Moscow, Russia*

## Abstract

Processes of heavy quark photoproduction at HERA energies are considered using the semihard ( $k_{\perp}$  factorization) QCD approach with emphasis of the BFKL dynamics of gluon distributions. We investigate the dependences of the total cross section of heavy quark photoproduction and also  $p_T$ , and rapidity distributions on different forms of the unintegrated gluon distribution. We present a comparison of the theoretical results with available H1 and ZEUS experimental data for charm and beauty photoproductions.

---

<sup>1</sup>Electronic address: artem\_lipatov@mail.ru

<sup>2</sup>Electronic address: saleev@info.ssu.samara.ru

<sup>3</sup>Electronic address: zotov@theory.npi.msu.su

# 1 Introduction

Recently, H1 and ZEUS Collaborations have reported [1, 2] experimental data on the total cross section of inelastic open beauty photoproduction. A comparison of these results with NLO pQCD calculations shows that ones underestimate the cross section at HERA energies. Therefore, it would be certainly reasonable to try a different way.

In the present note, we focus on the so called semihard approach [3, 4] (SHA), which we had applied earlier to open heavy quark [5] and  $J/\Psi$  [6, 7] photoproduction.

At the HERA energies and beyond, the interaction dynamics is governed by the properties of parton distributions in the small  $x$  region. This domain is characterized by the double inequality  $s \gg \mu^2 \simeq \hat{s} \gg \Lambda^2$ , which shows that the typical parton interaction scale  $\mu$  (mass  $m_c$  or  $p_T$  of heavy quark) is much higher than the QCD parameter  $\Lambda$ , but is much lower than the total c.m.s. energy  $\sqrt{s}$ . The situation is therefore classified as “semihard”.

The resummation [3, 4, 8, 9] of the terms  $[\ln(\mu^2/\Lambda^2) \alpha_s]^n$ ,  $[\ln(\mu^2/\Lambda^2) \ln(1/x) \alpha_s]^n$  and  $[\ln(1/x) \alpha_s]^n$  in SHA results in the unintegrated parton distributions  $\Phi_i(x, q_T^2, \mu)$ , which determine the probability to find a parton of type  $i$  carrying the longitudinal momentum fraction  $x$  and transverse momentum  $q_T$  at the probing scale  $\mu^2$ . They obey the BFKL equation [10] and reduce to the conventional parton densities  $F_i(x, \mu^2)$  once the  $q_T$  dependence is integrated out:

$$\int_0^{\mu^2} \Phi_i(x, q_T^2, \mu^2, Q_0^2) dq_T^2 = x F_i(x, \mu^2, Q_0^2). \quad (1)$$

To calculate the cross section of a physical process, the unintegrated functions  $\Phi_i$  have to be convoluted with off-mass shell matrix elements corresponding to the relevant partonic subprocesses. In the off-mass shell matrix element the virtual gluon polarization tensor is taken in the form of the SHA prescription [3, 4]:

$$L_{\mu\nu}^{(g)} = \overline{\epsilon_2^\mu \epsilon_2^{*\nu}} = p^\mu p^\nu x^2 / |q_T|^2 = q_T^\mu q_T^\nu / |q_T|^2 \quad (2)$$

In ref. [5] was used phenomenological parametrization for the unintegrated gluon distribution including an arbitrary normalization constant ( $K$ -factor), which was obtained from a fit to  $b\bar{b}$ -pair production at the Tevatron [4]. In our recent paper [7] we investigate the sensitivity of heavy quarkonium photoproduction to different gluon distributions. Special attention was given to the unintegrated gluon distributions obtained from BFKL evolution equation. In this paper we study the sensitivity of the total cross section of inelastic charm and beauty photoproduction to these unintegrated gluon distributions. The outline of our paper is the following: In sect. 2, we give the formulas for the cross sections of heavy quark photoproduction in the SHA of QCD. Then, in sect. 3, we describe the unintegrated distributions which we use for our calculations. In sect. 4, we present the results of our calculations. Finally, in sect. 5, we give some conclusions.

## 2 SHA QCD cross section for heavy quark photoproduction

We calculate the total and differential cross sections (the  $p_\perp$  and rapidity distributions) of charm and beauty quark photoproduction via the photon-gluon fusion QCD subprocess

(Fig.1) in the framework of the SHA.

First of all we take into account the transverse momentum of gluon  $\vec{q}_{2\perp}$ , its the virtuality  $q_2^2 = -\vec{q}_{2\perp}^2$  and the alignment of its polarization vectors along its transverse momentum such as  $\epsilon_\mu = q_{2\perp\mu} / |\vec{q}_{2\perp}|$  [3, 4, 8, 9]. Let us define Sudakov variables of the process  $ep \rightarrow Q\bar{Q}X$  (Fig.1):

$$\begin{aligned} p_1 &= \alpha_1 P_1 + \beta_1 P_2 + p_{1\perp} & p_2 &= \alpha_2 P_1 + \beta_2 P_2 + p_{2\perp} \\ q_1 &= x_1 P_1 + q_{1\perp} & q_2 &= x_2 P_2 + q_{2\perp} \end{aligned} \quad (3)$$

where

$$p_1^2 = p_2^2 = M^2, \quad q_1^2 = q_{1\perp}^2, \quad q_2^2 = q_{2\perp}^2,$$

$p_1$  and  $p_2$  are 4-momenta of the heavy quarks,  $q_1$  is 4-momentum of the photon,  $q_2$  is 4-momentum of the gluon,  $p_{1\perp}$ ,  $p_{2\perp}$ ,  $q_{1\perp}$ ,  $q_{2\perp}$  are transverse 4-momenta of these ones. In the center of mass frame of colliding particles we can write  $P_1 = (E, 0, 0, E)$ ,  $P_2 = (E, 0, 0, -E)$ , where  $E = \sqrt{s}/2$ ,  $P_1^2 = P_2^2 = 0$  and  $(P_1 P_2) = s/2$ . Sudakov variables are expressed as follows:

$$\begin{aligned} \alpha_1 &= \frac{M_{1\perp}}{\sqrt{s}} \exp(y_1^*) & \alpha_2 &= \frac{M_{2\perp}}{\sqrt{s}} \exp(y_2^*) \\ \beta_1 &= \frac{M_{1\perp}}{\sqrt{s}} \exp(-y_1^*) & \beta_2 &= \frac{M_{2\perp}}{\sqrt{s}} \exp(-y_2^*), \end{aligned} \quad (4)$$

where  $M_{1,2\perp}^2 = M^2 + p_{1,2\perp}^2$ ,  $y_{1,2}^*$  are rapidities of heavy quarks,  $M$  is heavy quark mass.

From conservation laws we can easily obtain the following conditions:

$$q_{1\perp} + q_{2\perp} = p_{1\perp} + p_{2\perp}, \quad x_1 = \alpha_1 + \alpha_2, \quad x_2 = \beta_1 + \beta_2 \quad (5)$$

The differential cross section of heavy quark photoproduction has the following form

$$\frac{d\sigma}{d^2 p_{1\perp}}(\gamma p \rightarrow Q\bar{Q}X) = \int dy_1^* \frac{d^2 q_{2\perp}}{\pi} \frac{\Phi_p(x_2, q_{2\perp}^2) |\bar{M}|^2}{16\pi^2 (sx_2)^2 \alpha_2} \quad (6)$$

The matrix element  $\bar{M}$  for a subprocess  $\gamma g^* \rightarrow q\bar{q}$  depends on the virtuality of the gluon and differs from the one of the usual parton model. For the square of this matrix element we used the following form [8]:

$$|\bar{M}|^2 = 16\pi^2 e_Q^2 \alpha_s \alpha_{em} (x_2 s)^2 \left[ \frac{\alpha_1^2 + \alpha_2^2}{(\hat{t} - M^2)(\hat{u} - M^2)} - \frac{2M^2}{q_T^2} \left( \frac{\alpha_1}{\hat{u} - M^2} - \frac{\alpha_2}{\hat{t} - M^2} \right)^2 \right], \quad (7)$$

where  $\hat{s}$ ,  $\hat{t}$ ,  $\hat{u}$  are usual Mandelstam variables of partonic subprocess  $\gamma g^* \rightarrow q\bar{q}$ .

### 3 Unintegrated gluon distribution

In this paper we used the different parametrizations for the unintegrated gluon distribution. First, as in the publication [5], we used the following phenomenological parametrization (LRSS-parametrization) [3, 4]:

$$\Phi(x, \vec{q}_T^2) = \Phi_0 \frac{0.05}{0.05 + x} (1-x)^3 f_1(x, \vec{q}_T^2), \quad (8)$$

where

$$f_1(x, \vec{q}_T^2) = \begin{cases} 1, & \text{if } \vec{q}_T^2 \leq q_0^2(x), \\ (q_0^2(x)/\vec{q}_T^2)^2, & \text{if } \vec{q}_T^2 > q_0^2(x) \end{cases} \quad (9)$$

with  $q_0^2(x) = q_0^2 + \Lambda^2 \exp(3.56\sqrt{\ln(x_0/x)})$ ,  $q_0^2 = 2\text{GeV}^2$ ,  $\Lambda = 56\text{MeV}$ ,  $x_0 = 1/3$ . The value of the parameter  $q_0^2(x)$  can be considered as a new typical transverse momentum of the partons in the parton cascade which leads to natural infrared cut-off in semihard approach. The normalization factor  $\Phi_0$  of the structure function  $\Phi(x, \vec{q}_T^2)$  was obtained in [4], where beauty production at CDF energy was described,  $\Phi_0 = 0.97 \text{ mb}$ .

The effective gluon distribution  $xG(x, \mu^2)$ , which was obtained from eq. (7)-(8), and eq. (1) increases at not very low  $x(0.01 < x < 0.15)$  as

$$xG(x, \mu^2) \sim x^{-\Delta}, \quad (10)$$

where  $\Delta \approx 0.5$  corresponds to the QCD pomeron singularity given by summation of leading logarithmic contributions  $(\alpha_s \ln \frac{1}{x})^n$  [10]. This increase continues up to  $x = x_0$ , where  $x_0$  is a solution of the equation  $q_0^2(x_0) = \mu^2$ . In the region  $x < x_0$ , there is saturation of the gluon distribution function:  $xG(x, \mu^2) \approx \Phi_0 \mu^2$ .

A second parametrization is based on the numerical solution of the BFKL evolution equations [11] (RS-parametrization). The solution has the following form [11]:

$$\begin{aligned} \Phi(x, q^2) = & \frac{a_1}{a_2 + a_3 + a_4} [a_2 + a_3 (\frac{Q_0^2}{q^2}) + (\frac{Q_0^2}{q^2})^2 + \\ & \alpha x + \frac{\beta}{\epsilon + \ln(1/x)}] C_q [\frac{a_5}{a_5 + x}]^{1/2} [1 - \\ & a_6 x^{a_7} \ln(q^2/a_8)] (1 + a_{11}x)(1 - x)^{a_9 + a_{10} \ln(q^2/a_8)}, \end{aligned} \quad (11)$$

where

$$C_q = \begin{cases} 1, & \text{if } q^2 < q_0(x), \\ q_0(x)/q^2, & \text{if } q^2 > q_0(x). \end{cases} \quad (12)$$

All parameters (see [11]) ( $a_1 - a_{11}$ ,  $\alpha$ ,  $\beta$  and  $\epsilon$ ) were found by minimization of the differences between left hand and right-hand of the BFKL-type equation for unintegrated gluon distribution  $\Phi(x, q^2)$ ,  $Q_0^2 = 4 \text{ GeV}^2$ .

Finally we also use the results of a BFKL-like parameterization <sup>4</sup> of the unintegrated gluon distribution  $\Phi(x, q_T^2, \mu^2)$ , according to the prescription given in [12]. The proposed method lies upon a straightforward perturbative solution of the BFKL equation where the collinear gluon density  $xG(x, \mu^2)$  from the standard GRV set [12] is used as the boundary condition in the integral form (1). Technically, the unintegrated gluon density is calculated as a convolution of collinear gluon density  $G(x, \mu^2)$  with universal weight factors [12]:

$$\Phi(x, q_T^2, \mu^2) = \int_x^1 \mathcal{G}(\eta, q_T^2, \mu^2) \frac{x}{\eta} G(\frac{x}{\eta}, \mu^2) d\eta, \quad (13)$$

where

$$\mathcal{G}(\eta, q_T^2, \mu^2) = \frac{\bar{\alpha}_s}{\eta q_T^2} J_0(2\sqrt{\bar{\alpha}_s \ln(1/\eta) \ln(\mu^2/q_T^2)}), \quad q_T^2 < \mu^2, \quad (14)$$

---

<sup>4</sup> Of course LRSS and RS parametrizations are BFKL - type too.

$$\mathcal{G}(\eta, q_T^2, \mu^2) = \frac{\bar{\alpha}_s}{\eta q_T^2} I_0(2\sqrt{\bar{\alpha}_s \ln(1/\eta) \ln(q_T^2/\mu^2)}), \quad q_T^2 > \mu^2, \quad (15)$$

where  $J_0$  and  $I_0$  stand for Bessel functions (of real and imaginary arguments, respectively), and  $\bar{\alpha}_s = 3\alpha_s/\pi$ . The parameter  $\bar{\alpha}_s$  is connected with the Pomeron trajectory intercept:  $\Delta = \bar{\alpha}_s 4 \ln 2$  in the LO and  $\Delta = \bar{\alpha}_s 4 \ln 2 - N\bar{\alpha}_s^2$  in the NLO approximations, respectively, where  $N \sim 18$  [14]. The latter value of  $\Delta$  have dramatic consequences for high energy phenomenology. In particular it leads to negative values for physical cross sections [15]. However some resummation procedures proposed in the last years lead to positive value of  $\Delta$  ( $\sim 0.2 - 0.3$ ) [16, 17]. Therefore in our calculations with (13) we used only the solution of LO BFKL equation and considered  $\Delta$  as free parameter varying it from 0.166 to 0.53.

The presence of the two different parameters,  $\mu^2$  and  $q_T^2$ , in eq.(12) for unintegrated gluon distribution  $\Phi(x, q_T^2, \mu^2)$  refers to the fact that the evolution of parton densities proceeds in two steps. First the DGLAP scheme [18] is applied to evolve the structure function from  $Q_0^2$  to  $\mu^2$  within the collinear approximation. After that eqs. (12)-(14) are used to develop the parton transverse momenta  $q_T^2$  in correspondence with BFKL evolution [10].

This approach was used for the description of  $p_T$  spectrum of  $D^*$  meson electroproduction at HERA [19] and  $J/\Psi$  photoproduction [7], where in the first case for Pomeron intercept parameter was obtained the value  $\Delta = 0.35$ . However for the total cross section of inelastic  $J/\Psi$  photoproduction  $\Delta = 0.53$  is more preferable.

## 4 Results of calculations

The calculations of the heavy quark photoproduction cross section in the SHA have been made according to eqns. (6) and (7) for  $\vec{q}_T^2 > q_0^2 \text{ GeV}^2$  and for  $\vec{q}_T^2 \leq q_0^2 \text{ GeV}^2$  we set  $|\vec{q}_T| = 0$  in the matrix element of process and use one of the standard parton model (SPM). The choice of the critical value of parameter  $\vec{q}_T^2 = q_0^2 = 1 - 2 \text{ GeV}^2$  is determined by the requirement of the small value of  $\alpha_s(\vec{q}_T^2)$  in the region  $\vec{q}_T^2 > 1 - 2 \text{ GeV}^2$ , where in fact  $\alpha_s(\vec{q}_T^2) \leq 0.26$ <sup>5</sup>.

The results of our calculations for the cross sections of  $c\bar{c}$  and  $b\bar{b}$  photoproduction processes are shown in Figs. 2 - 10. Fig. 2 shows the total cross section of the inelastic  $c\bar{c}$  photoproduction at HERA and fixed target energies as a function of  $\sqrt{s}$ . The curves 3, 4 and 5 correspond to the SHA calculations with the RS, LRSS and BFKL unintegrated gluon distributions at the Pomeron intercept  $\Delta = 0.35$ ,  $m_c = 1.5 \text{ GeV}$  and at values of  $q_0^2 = 4, 2$  and  $1 \text{ GeV}^2$  accordingly. One can see that the SHA curves 4 and 5 describe the data better than the SPM ones (1 and 2). The RS parameterization of the unintegrated gluon distribution gives the total cross section more close to SPM result (obtained with GRV gluon density) because of very large value of  $q_0^2 = 4 \text{ GeV}^2$ .

The LRSS parameterization of the unintegrated gluon distribution gives the cross section which stops to increase at energy  $\sqrt{s} \geq 150 \text{ GeV}$  because of saturation effects accounted for by the parameterizations (8) and (9). We would like to stress that account for saturation

---

<sup>5</sup>The substitution  $q_0^2 = 1 \text{ GeV}^2$  instead  $2 \text{ GeV}^2$  essentially influences on the dependence of cross sections from the BFKL parameterization of unintegrated gluon distribution.

effects in the region  $x \leq 10^{-3}$  [5, 20], does not contradict the H1 and ZEUS experimental data [21, 22].

The BFKL parameterization (curve 5) describes the H1 and ZEUS data very well at  $m_c = 1.3$  GeV (Fig. 3) The curves 3, 4 and 5 obtained in the SHA show more rapid growth with energy than those obtained in the SPM with GRV [13](curve 2) and MT [23] (curve 1) parameterizations.

In Fig.4 we show the dependence of the total cross section from  $\Delta$  parameter for the BFKL parametrization (13) - (15) at  $m_c = 1.3$  GeV. The dependence is very weak in contrast with the dependence of the total inelastic  $J/\Psi$  photoproduction cross section [7].

The results of our calculations for the  $p_T$  and rapidity  $y$  ( $y = y_1^*$ ) distributions of the  $c$  quarks at  $\sqrt{s} = 200$  GeV are shown in Figs. 5 and 6. The SHA curves 4 and 5 in Fig. 5 for the  $p_T$  distribution are higher than those of the SPM. It is effect of the SHA broadening of  $p_T$  spectra due to extra transverse momentum of the initial gluons [4]- [6]. The SHA rapidity distributions (Fig. 6) have more similar behaviour in wide rapidity region.

Fig. 7 shows the total cross section of inelastic  $b\bar{b}$  photoproduction at HERA energies as a function of  $\sqrt{s}$ . The curves 3, 4 and 5 correspond to the SHA calculations with the RS, LRSS and BFKL unintegrated gluon distributions at the Pomeron intercept  $\Delta = 0.35$ ,  $m_b = 4.75$  GeV and at values of  $q_0^2 = 4, 2$  and  $1$  GeV<sup>2</sup> accordingly. The H1 [1] and EMC [24] experimental data are described by the LRSS parameterization (curve 4) and the BFKL parameterization (curve 5 in Fig. 8) but at small value of  $m_b = 4.25$  GeV only for the last parameterization.

The results of the SHA calculations for the  $p_T$  and rapidity distributions of the  $b$  quarks at  $\sqrt{s} = 200$  GeV are shown in Figs. 9 and 10. The differences between SHA curves and SPM ones are more pronounced than in the  $c$ -quark case.

## 5 Conclusions

We considered the process of inelastic heavy quark photoproduction at HERA in the framework of the semihard QCD approach with emphasis on the BFKL dynamics of gluon distributions. We investigated total cross section of inelastic  $c$ - and  $b$ -quark photoproduction and also  $p_T$  and rapidity spectra as a function of different unintegrated gluon distributions. It is shown that the description of the  $c$ -quark inelastic cross section at HERA energies is achieved in the cases of the LRSS and BFKL parameterizations at  $\Delta = 0.35$ <sup>6</sup> and at the values of  $m_c = 1.5$  and  $1.3$  GeV and at  $q_0^2 = 2$  and  $1$  GeV<sup>2</sup> accordingly.

The cross section of inelastic  $b$ -quark photoproduction at HERA is described by the LRSS parameterization at the value of  $m_b = 4.75$  GeV and  $\Delta = 0.35$  very well. The BFKL parameterization with  $\Delta = 0.35$  describes the H1 and EMC experimental data at  $m_b = 4.25$  GeV only.

The dependence of the total cross section of inelastic open  $c$ - and  $b$ -quark photoproduction on  $\Delta$  parameter for the BFKL parameterization (13) - (15) is very weak in contrast with the dependence of the total inelastic  $J/\Psi$  photoproduction cross section.

---

<sup>6</sup> Close values for the parameter  $\Delta$  were obtained rather in very different papers (see, for example, [25]-[28]) and in the L3 experiment [29].

## 6 Acknowledgments

One of us (N.Z.) would like to thank S. Baranov and H. Jung for numerous discussions of different aspects of the QCD SHA, the Elementary Particle Department of Institute of Physics of Lund University and specially Leif Jönsson for their warm hospitality and the Theoretical Department of Institute of Physics of Lund University for very useful discussions. This work has been supported in part by the Royal Swedish Academy of Sciences.

## References

- [1] H1 Collaboration, C. Adloff et al., *Phys. Lett.* **B467** (1999) 156.
- [2] ZEUS Collaboration, paper 498, submitted to the Intern. Europhysics Conference on H.E. Physics, Tampere, Finland, 1999.
- [3] L.V. Gribov, E.M. Levin, M.G. Ryskin, *Phys. Rep.* **100** (1983) 1.
- [4] E.M. Levin, M.G. Ryskin, Yu.M. Shabelski, A.G. Shuvaev, *Sov. J. Nucl. Phys.* **53** (1991) 657.
- [5] V.A. Saleev, N.P. Zotov N.P., *Mod. Phys. Lett.* **A11** (1996) 25.
- [6] V.A. Saleev, N.P. Zotov, *Mod. Phys. Lett.* **A9** (1994) 151; 1517.
- [7] A.V. Lipatov, N.P. Zotov, *Mod. Phys. Lett.* **A15** (2000) 695.
- [8] S. Catani, M. Ciafoloni, F. Hautmann, *Nucl. Phys.* **B366** (1991) 135.
- [9] J.C. Collins and R.K. Ellis, *Nucl. Phys.* **B360** (1991) 3.
- [10] E. Kuraev, L. Lipatov, V. Fadin, *Sov. Phys. JETP* **44** (1976) 443.  
E. Kuraev, L. Lipatov, V. Fadin, *Sov. Phys. JETP* **45** (1977) 199.  
Y. Balitskii, L. Lipatov, *Sov. J. Nucl. Phys.* **28** (1978) 822.
- [11] M.G. Ryskin, Yu.M. Shabelski, *Z. Phys.* **C61** (1994) 517; **C66** (1995) 151.
- [12] J. Blumlein, DESY 95-121.
- [13] M. Gluck, E. Reya, A. Vogt, *Z. Phys.* **C67** (1995) 433.
- [14] D.A. Ross, *Phys. Lett* **B431** (1998) 161, hep-ph/9804332.
- [15] E. Levin, hep-ph/9806228.
- [16] G. Salam. *JHEP* **9807:019** (1998), hep-ph/9806482.
- [17] S.J. Brodsky, V.S. Fadin, V.T. Kim, L.N. Lipatov, G.B. Pivovarov, *JETP Lett.* **70** (1999) 155, hep-ph/9901229.

- [18] V. Gribov, L. Lipatov, *Sov. J. Nucl. Phys.* **15** (1972) 438 and 675.  
L. Lipatov, *Sov. J. Nucl. Phys.* **20** (1975) 94.  
G. Altarelli, G. Parisi, *Nucl. Phys.* **B126** (1977) 298.  
Y. Dokshitzer, *Sov. Phys. JETP* **46** (1977) 641.
- [19] S. P. Baranov, N.P. Zotov, *Phys. Lett.* **B458** (1999) 389.
- [20] V.A. Saleev, N.P. Zotov, in *Proceeding of the Workshop DIS'96*, p. 318.
- [21] H1 Collaboration, S. Aid et al., *Nucl. Phys.* **B472** (1996) 32.
- [22] ZEUS Collaboration, M. Derrick et al., *Phys. Lett.* **B349** (1995) 225.
- [23] J. Morfin, Wu-Ki Tung, *Z. Phys.* **C52** (1991) 13.
- [24] EMC, J.-J. Aubert et al. *Phys. Lett.* **B106** (1981) 419.
- [25] J. Kwiecinski, A.D. Martin, P.J. Sutton, *Z. Phys.* **C71** (1996) 585.
- [26] B. Andersson, G. Gustafson, H. Kharrazina, J. Samuelsson, *Z. Phys.* **C71** (1996) 613.
- [27] N.N. Nikolaev, V.R. Zoller, hep-ph/0001084.
- [28] B.I. Ermolaev, M.Greco, S.I. Troyan, Preprint CERN-TH/99-155.
- [29] L3 Collaboration, M. Acciarri et al., *Phys. Lett.* **B453** (1999) 333.



## Figure captions

**Fig. 1** QCD diagram for the open heavy quark electroproduction.

**Fig. 2** The total cross section of inelastic  $c\bar{c}$  photoproduction as a function  $\sqrt{s}$  at  $m_c = 1.5$  GeV.

**Fig. 3** The total cross section of inelastic  $c\bar{c}$  photoproduction as a function  $\sqrt{s}$  at  $m_c = 1.3$  GeV.

**Fig. 4** The total cross section of inelastic  $c\bar{c}$  photoproduction as a function  $\sqrt{s}$  at  $m_c = 1.3$  GeV and different values of  $\Delta$ : **1** -  $\Delta = 0.166$ , **2** -  $\Delta = 0.35$ , **3** -  $\Delta = 0.53$ .

**Fig. 5** The  $p_T^2$  distribution of inelastic  $c\bar{c}$  photoproduction at  $\sqrt{s} = 200$  GeV.

**Fig. 6** The rapidity distribution of inelastic  $c\bar{c}$  photoproduction at  $\sqrt{s} = 200$  GeV.

**Fig. 7** The total cross section of inelastic  $b\bar{b}$  photoproduction as a function  $\sqrt{s}$  at  $m_b = 4.75$  GeV.

**Fig. 8** The total cross section of inelastic  $b\bar{b}$  photoproduction as a function  $\sqrt{s}$  at  $m_b = 4.25$  GeV.

**Fig. 9** The  $p_T^2$  distribution of inelastic  $b\bar{b}$  photoproduction at  $\sqrt{s} = 200$  GeV.

**Fig. 10** The rapidity distribution of inelastic  $b\bar{b}$  photoproduction  $\sqrt{s} = 200$  GeV.

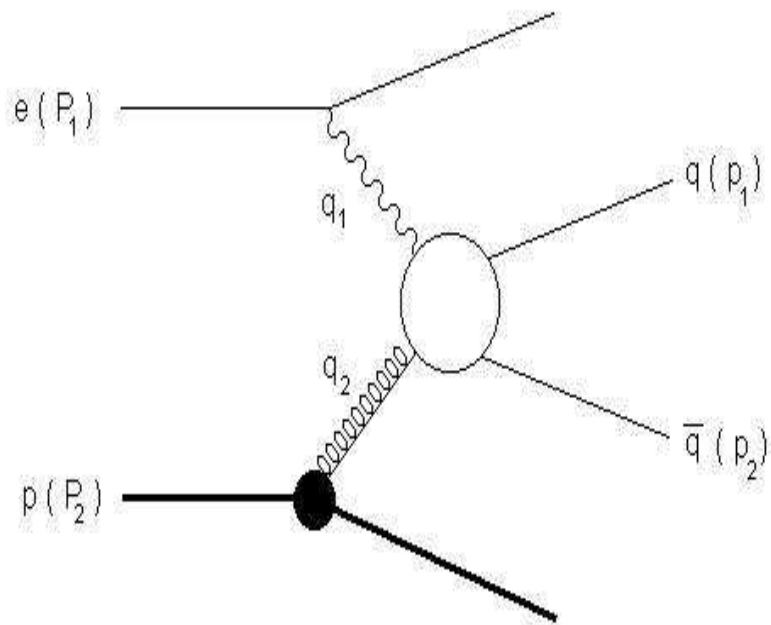


Fig. 1.

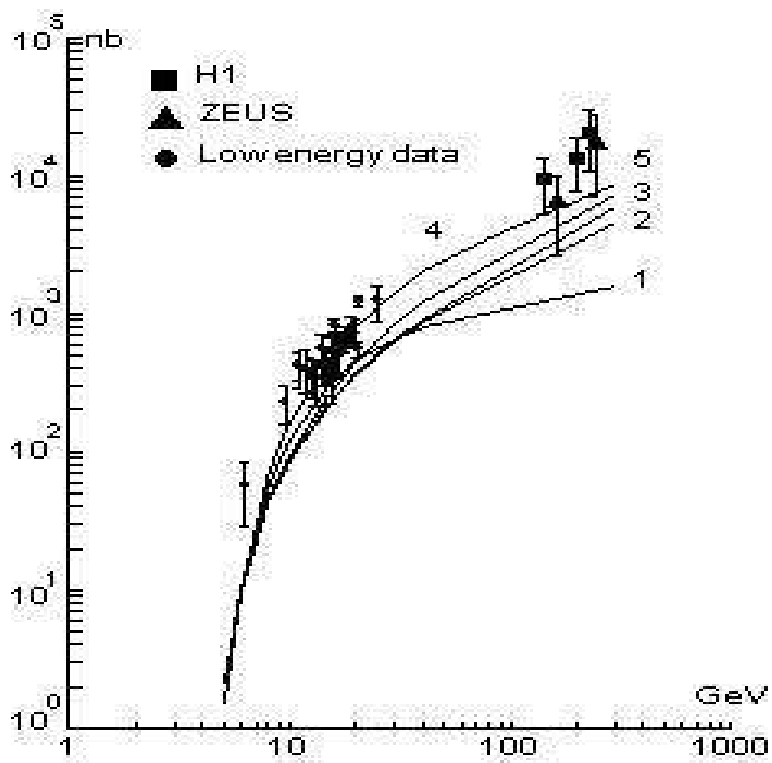


Fig. 2.

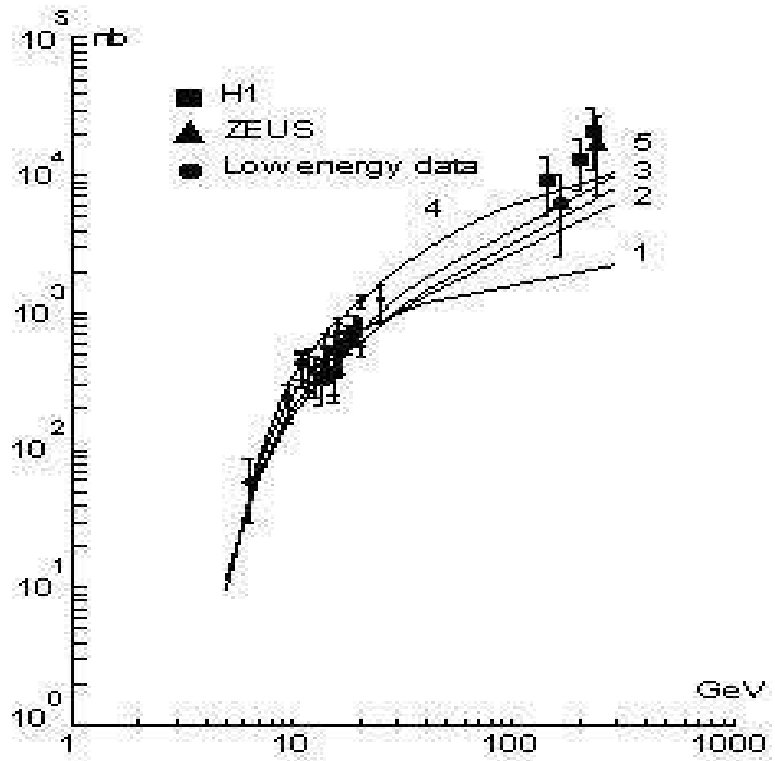


Fig. 3.

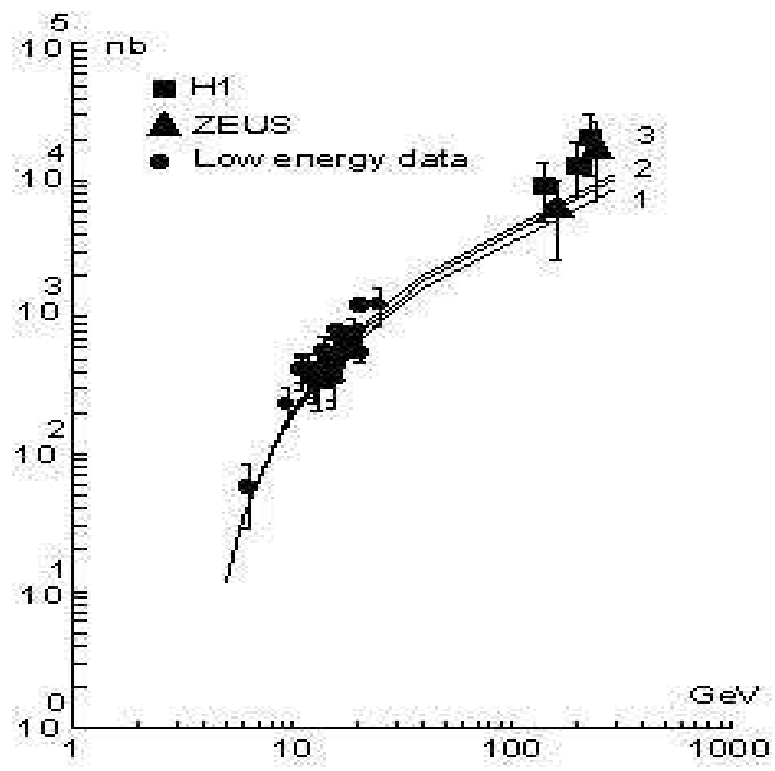


Fig. 4.

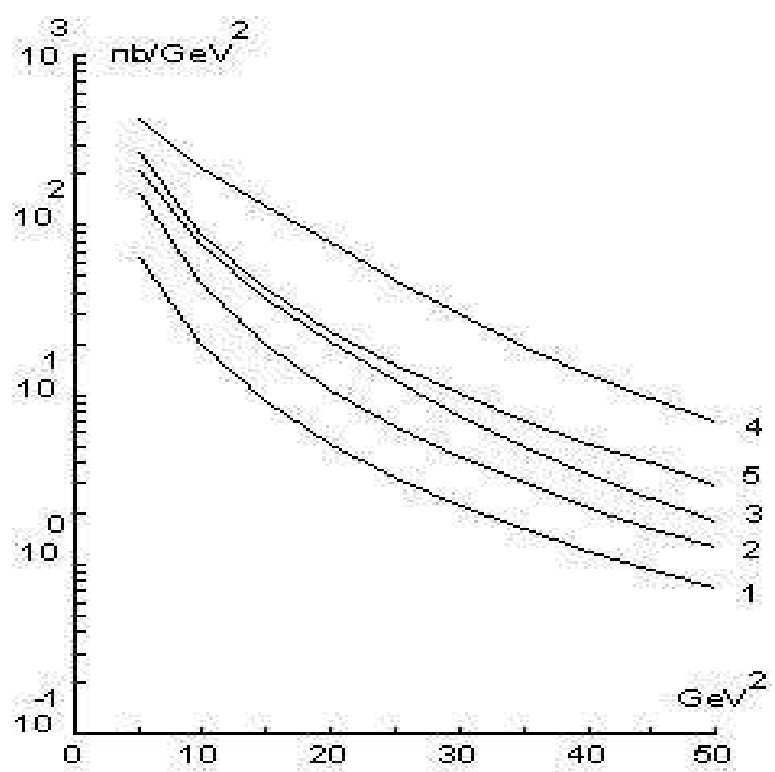


Fig. 5.

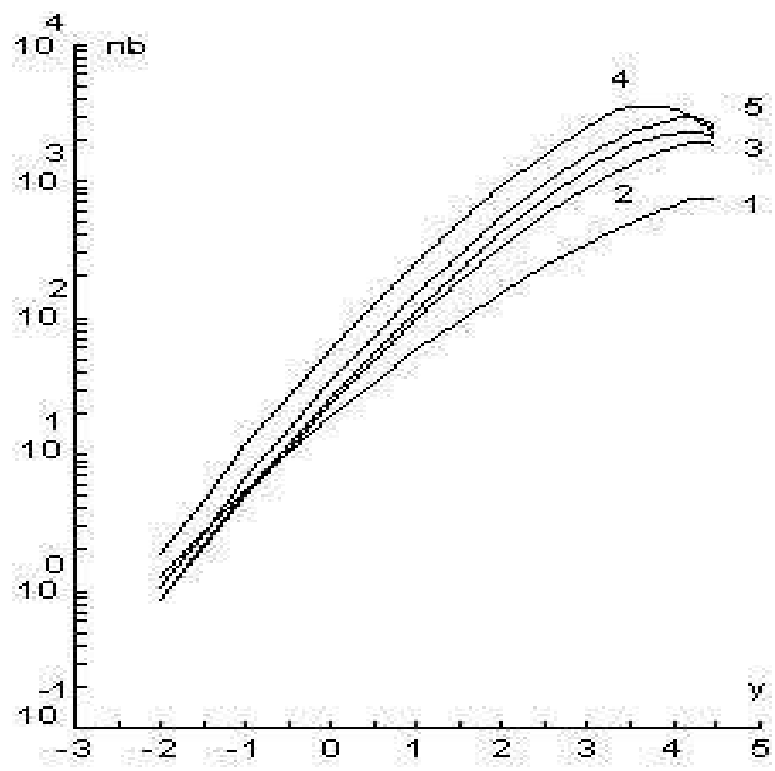


Fig. 6.

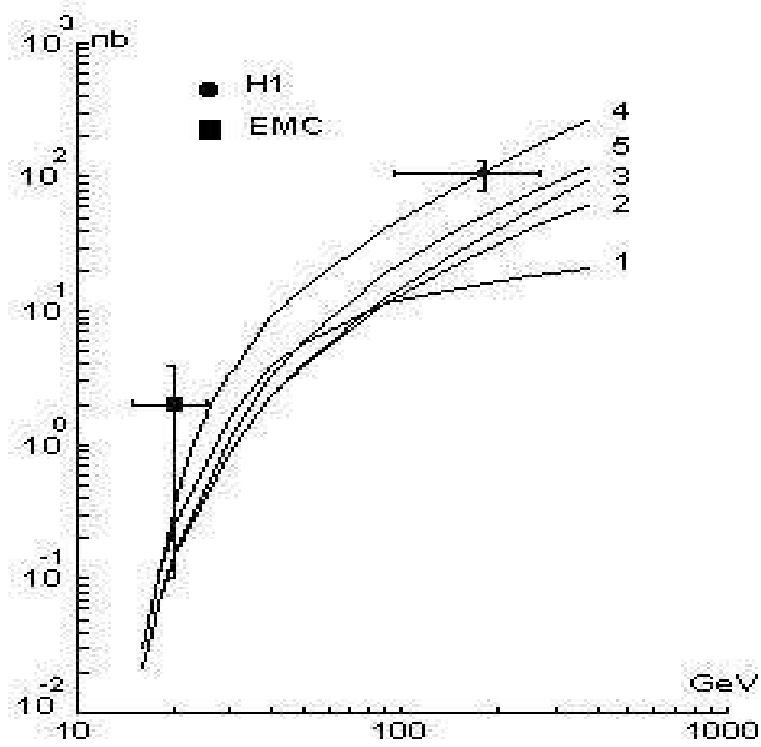


Fig. 7.

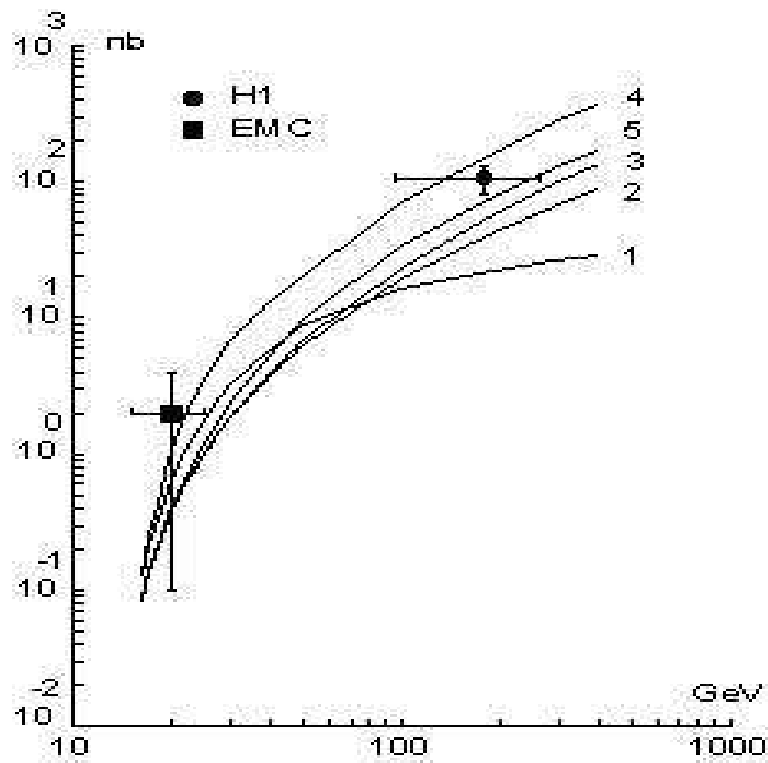


Fig. 8.

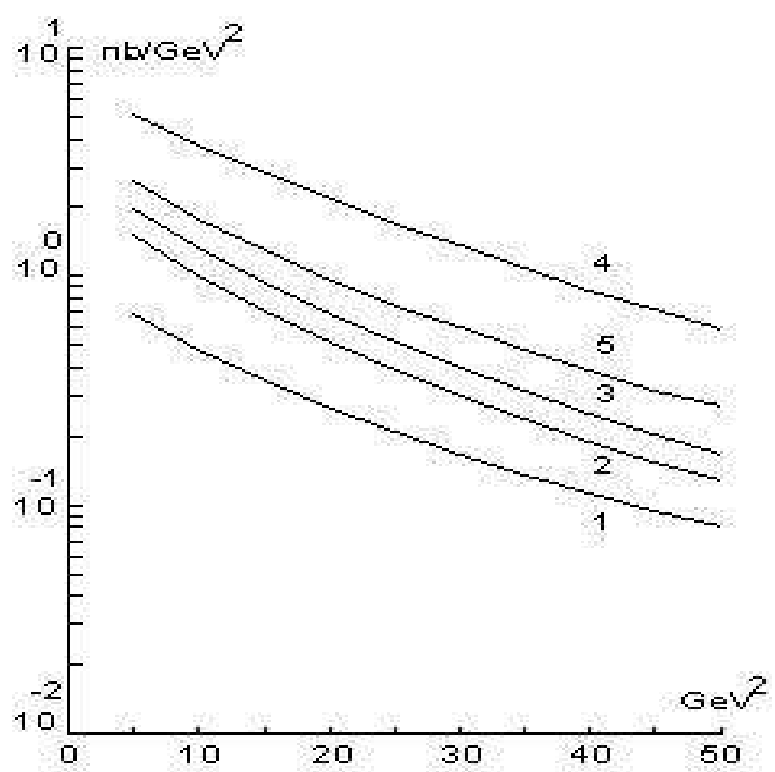


Fig. 9.

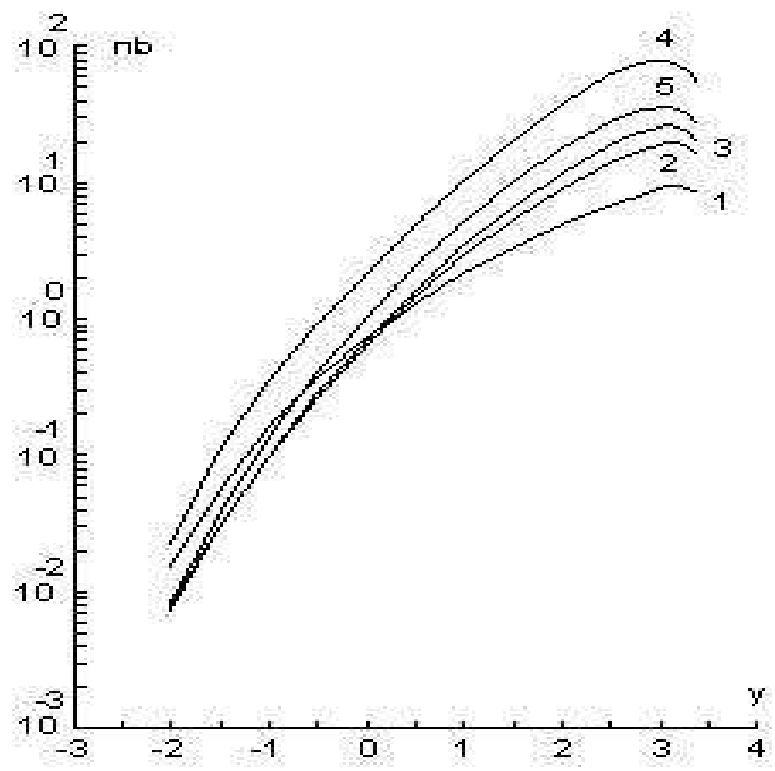


Fig. 10.